Synthesis, packing arrangement and transistor performance of dimers of dithienothiophenes†

Lei Zhang, Lin Tan, Wenping Hu and Zhaohui Wang*

Received 7th July 2009, Accepted 4th September 2009
First published as an Advance Article on the web 25th September 2009
DOI: 10.1039/b913340b

We present the synthesis, characterization, and transistor performance of a series of semiconductor materials based on dimers of dithienothiophenes with different linkages. The relationship between molecular structure, molecular packing arrangement, film morphology, and device performance has been investigated. Subtle changes in molecular structure lead to dramatically different packing modes in the solid state and greatly affect the transport properties of the carriers. The FET devices based on the vinylene-bridged dimers **4** and **5** show mobilities up to 0.08 $cm^2 V^{-1} s^{-1}$ and 0.89 $cm^2 V^{-1} s^{-1}$ respectively.

Introduction

Organic field-effect transistors (OFETs) are of great interest for applications such as identification tags, smart cards and flexible displays.[1,2] Until now, there has been great progress in both the development of new semiconductors and new fabrication techniques. Some OFETs even exhibit performances exceeding their inorganic counterparts (amorphous silicon devices).[3–5] Among these materials, oligo- and polythiophenes are heavily studied systems due to their synthetic accessibility, broad structural diversity, and good film properties.[6–8] However, one drawback of this class of polymer is that they are prone to photo-oxidation and doping, which produce a significant drop in their performance.[9,10] Therefore, various strategies have been explored to change the backbone microstructure and the energy levels of the molecular orbitals.[11–14] For example, inclusion of a conjugated unit, which has a large resonance stabilization, will reduce the conjugation of the backbone and increase ionization potential (IP). Recently, McCulloch *et al.* reported that incorporation of thienothiophene units into a polythiophene backbone resulted in an increase in IP but did not perturb the regioregularity of pendant alkyl side chains along the backbone. Mobilities as high as 0.6 $cm^2V^{-1}s^{-1}$ have been measured.[12] However, there remains a challenge to increase the polymer IP without disturbing the close molecular aggregation that facilitates high carrier mobility.

In contrast to polythiophenes, fused-ring thienoacenes have large band gaps due to the greater resonance stabilization energy of the fused ring over the single thiophene ring.[15–18] Furthermore, this extended π system is decorated with S atoms, which can enhance intermolecular overlaps and facilitate carrier migration.[19–22] However, OFETs based on fused-ring thienoacenes have received limited study due to their tedious synthesis and the low solubility of such compounds.

Dithienothiophenes are precursors for highly fused thiophene compounds and can be effectively synthesized from commercial 3-bromothiophene.[15,23] Furthermore, dithieno[3,2-*b*:2′,3′-*d*]thiophenes are potential candidates for organic electronics, and materials based on dithieno[3,2-*b*:2′,3′-*d*]thiophenes have shown high field-effect transistor characteristics due to the strong orbital overlap which can strongly affect the rate of intermolecular hopping.[24–27] Compared with dithieno[3,2-*b*:2′,3′-*d*]thiophenes, dithieno[2,3-*b*:3′,2′-*d*]thiophenes (β-trithiophenes) are characterised by a lower degree of delocalization, owing to the fact that the terminal rings are joined by a bond connecting two carbons β to sulfur. With the central cross-conjugated double bonds, this compound is usually chosen as a building block for helical β-oligothiophenes.[28–31] We first chose dithieno[2,3-*b*:3′,2′-*d*]thiophene as a building block in OFETs because of its ability to facilitate short intermolecular S···S interactions and pave a way to investigate the relationship between structure and electronic properties. Recently, we reported some novel high performance organic semiconductors based on β-trithiophene units, which exhibit unique molecular packing motifs and good device performance.[32,33] To better understand the relationship between the molecular crystal structure, film morphology, and device characteristics, in this contribution we present the detailed synthesis and characterization of a series of organic semiconductors based on dithieno[3,2-*b*:2′,3′-*d*]thiophenes and dithieno[2,3-*b*:3′,2′-*d*]thiophene building blocks with different linkages (Fig. 1).

Experimental

Material and general methods

General: ^{1}H NMR and ^{13}C NMR spectra were recorded in deuterated solvent on a Bruker AVANCE 400 NMR spectrometer and a Bruker AVANCE 600 NMR. ^{1}H NMR chemical shifts were reported in ppm downfield from tetramethylsilane (TMS) reference using the residual protonated solvent as an internal standard. EI-MS spectra were obtained on a Shimadzu QP-2010

National Laboratory for Molecular Science, Key Laboratory of Organic Solid, Institute of Chemistry, Chinese Academy of Science Beijing, 100190, P. R. China. E-mail: wangzhaohui@iccas.ac.cn; Fax: +86 62650811; Tel: +86 62650811

† Electronic supplementary information (ESI) available: UV-vis spectra of compound **1**, **2**, **5**; CV spectra of all the compounds; DSC, TGA measurement of all the compounds. CCDC reference number 680799 (compound **4**). For ESI and crystallographic data in CIF or other electronic format see DOI: 10.1039/b913340b

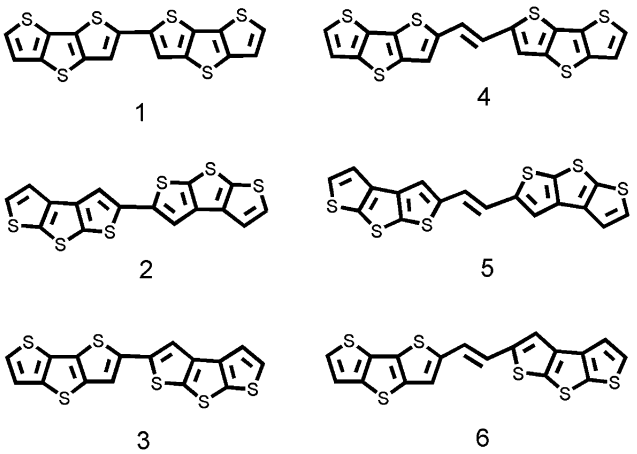

Fig. 1 Chemical structures of dimers of dithienothiophenes.

spectrometer and MALDI-TOF-MS were determined on a Bruker BIFLEX Mass spectrometer. All chemicals were purchased from commercial suppliers and used without further purification unless otherwise specified. THF was freshly distilled from sodium prior to use. The syntheses of dimers of dithieno[3,2-*b*:2′,3′-*d*]thiophene (**1**), α,α′-bis(dithieno [2,3-*b*:3′,2′-*d*]thiophene) (**2**), *trans*-1,2-(dithieno[2,3-*b*:3′,2′-*d*] thiophene)ethene (**5**), 5-bromodithieno[2,3-*b*:3′,2′- *d*]thiophene, and dithieno[2,3-*b*:3′,2′-*d*]thiophene-5-carbaldehyde have already been reported in the literature.[24,32]

FET devices were fabricated in the top contact geometry configuration. Thin films were deposited under vacuum on octadecyl-trichlorosilane (OTS) modified silicon oxide layers. Gold electrodes were deposited using shadow masks with a length-to-width ratio (*L*/*W*) of *ca.* 48.2/1. Organic semiconductors were deposited at an initial rate of 0.1 $Å s^{-1}$ then increasing to 0.4–0.6 $Å s^{-1}$ gradually under a pressure of about 4.0×10^{-6} Torr to a final thickness of 60 nm as determined by a quartz crystal monitor. FET characteristics were obtained at room temperature in air on a Keithley 4200 SCS and Micromanipulator 6150 probe station. The mobility of the devices based on the fused-ring oligomers was calculated in the saturation regime. The equation used is as follows:

$$I_{DS} = (W/2L)C_i\mu(V_{GS} - V_T)^2$$

where *W*/*L* is the channel width/length, C_i is the insulator capacitance per unit area, V_{GS} and V_T are the gate voltage and threshold voltage, respectively.

Materials synthesis

2-(Tri-*n*-butylstannyl)dithieno[3,2-*b*:2′,3′-*d*]thiophene (7). *n*-BuLi (5.4 mmol) was added dropwise to a solution of dithieno[3,2-*b*:2′,3′-*d*]thiophene (1 g, 5.1 mmol) in THF (50 ml) at −78 °C. After stirring for 3 h at −78 °C, tri-*n*-butyltin chloride (2.5 g, 7.7 mmol) was added. The reaction mixture was then gradually warmed to room temperature and stirred overnight. The solution was quenched with water and extracted with diethyl ether several times. The combined organic phases were washed with saturated brine, dried over $MgSO_4$ and concentrated in vacuo. The crude product was directly used in the subsequent reaction.

5-Dithieno[2,3-*b*:3′,2′-*d*]thiophene-2-dithieno[3,2-*b*:2′,3′-*d*]thiophene (3). A solution of 5-bromodithieno[2,3-*b*:3′,2′-*d*]thiophene (0.5 g, 1.8 mmol), tetrakis(triphenylphosphine)palladium (0.17 g, 0.15 mmol), and 2-(tri-*n*-butylstannyl)dithieno[2,3-*b*:3′, 2′-*d*]thiophene (0.8 g, 1.62 mmol) in toluene (100 ml) was refluxed at 125 °C for 12 h under argon. The reaction mixture was cooled to room temperature, purified by chromatography (petroleum/dichloromethane 1:1) on a short column and then sublimed to give a yellow solid (0.30 g, 48%). Mp: 218 °C; ^{1}H NMR (400 MHz, $CDCl_3$) δ 7.49 (s, 1H), 7.42 (d, 1H, J = 5.2 Hz), 7.40 (d, 2H, J = 1.3 Hz), 7.38 (d, 1H, J = 1.3 Hz), 7.30 (d, 1H, J = 5.2 Hz); MS (MALDI-TOF) 389.4; Anal. Calcd for $C_{16}H_6S_6$: C, 49.20%; H, 1.55%. Found: C, 49.00%; H, 1.77%.

5-Hydroxymethyldithieno[2,3-*b*:3′,2′-*d*]thiophene (8). To a solution of dithieno[2,3-*b*:3′,2′-*d*]thiophene-5-carbaldehyde (1 g, 4.5 mmol) in THF/ethanol (100 ml, 1:1), sodium borohydride (0.68 g, 18 mmol) was added. The mixture was stirred at room temperature for 3 h, then diethyl ether was added and the organic layer was washed with water, dried with $MgSO_4$, and purified on a short column using dichloromethane as eluent to give white crystals (1.0 g, 99%). Mp: 135–137 °C; ^{1}H NMR (400 MHz, $CDCl_3$) δ 7.39 (d, 1H, J = 5.2 Hz), 7.33 (d, 1H, J = 5.2 Hz), 7.29 (s, 1H), 4.89 (s, 2H); ^{13}C NMR (600 MHz, $CDCl_3$) δ 146.7, 138.9, 138.6, 138.5, 137.6, 127.7, 118.8, 117.3, 60.8; MS (EI) m/z = 226 (M^+); Anal. Calcd for $C_9H_6OS_3$: C, 47.76%; H, 2.67%. Found: C, 47.83%; H, 2.80%.

(Dithieno[2,3-*b*:3′,2′-*d*]thiophene-2-methyl)triphenylphosphonium bromide (9). To a solution of 5-hydroxymethyldithieno[2,3-*b*:3′,2′-*d*]thiophene (0.7 g, 3.1 mmol) in acetonitrile (50 ml), triphenylphosphine hydrobromide (1.3 g, 3.7 mmol) was added at room temperature and the reaction mixture refluxed for 3 h. The resultant white suspension was cooled and filtered. The solid was washed with diethyl ether several times and dried to give a white solid (1.7 g, 100%). ^{1}H NMR (400 MHz, $CDCl_3$) δ 7.85–7.70 (m, 9H), 7.64 (t, 7H, J = 3.5 Hz), 7.30 (d, 1H, J = 5.2 Hz), 7.25 (d, 1H, J = 5.2 Hz), 6.10 (d, 2H, J = 5.2 Hz); ESI (+Br) m/z = 551.1.

***trans*-1-(5-Dithieno[2,3-*b*:3′,2′-*d*]thiophene)-2-(2-dithieno[3,2-*b*:2′,3′-*d*]thiophene)ethene (6).** To a solution of dithieno [3,2-*b*:2′,3′-*d*]thiophene-2-carbaldehyde[34] (0.5 g, 2.2 mmol) and (dithieno[2,3-*b*:3′,2′-*d*]thiophene-2-methyl)triphenylphosphonium bromide (1.3 g, 2.2 mmol) in THF (100 ml), t-BuOK (0.42 g, 3.3 mmol) was added slowly. The mixture was stirred at room temperature for 5 h and the yellow suspension was filtered. The solid was washed with water, acetone, dichloromethane, and sublimed to give a yellow solid (0.69, 66%). Mp: 260 °C; ^{1}H NMR (400 MHz, $CDCl_3$) δ 7.41 (d, 1H, J = 5.2 Hz), 7.38 (d, 1H, J = 5.2 Hz), 7.36 (dd, 1H, J = 5.2 Hz), 7.32 (s, 1H), 7.30 (d, 1H, J = 5.2 Hz), 7.38 (s, 1H), 7.08 (d, 2H, J = 4.2 Hz); MS (MALDI-TOF) 415.9; Anal. Calcd for $C_{18}H_8S_6$: C, 51.89%; H, 1.94%. Found: C, 51.69%; H, 2.04%.

***trans*-1,2-Bis(dithieno[3,2-*b*:2′,3′-*d*]thiophene)ethene (4).** To a suspension of zinc power (2.6 g, 41 mmol) in THF (60 ml), titanium tetrachloride (2.2 ml) was slowly added, and the resultant mixture heated at reflux for 3 h. A solution of aldehyde **10** (4.1 mmol) and pyridine (3.5 g) in THF (30 ml) was slowly added

to the mixture and the mixture was refluxed for 12 h. After cooling to room temperature, the mixture was diluted with saturated sodium hydrogen carbonate (500 ml) and stirred for 3 h. The solid was filtered and washed with diluted HCl, water, acetone and dried, then sublimed to give an orange solid (65%). Mp: 318 °C; MS (MALDI-TOF) 416.5; ^{1}H NMR (400 MHz, $CDCl_3$) δ 7.41 (d, 2H, $J = 5.2$ Hz), 7.61 (d, 2H, $J = 5.2$ Hz), 7.35 (s, 2H), 7.06 (d, 2H, $J = 4.2$ Hz); Anal. Calcd for $C_{18}H_8S_6$: C, 51.89%; H, 1.94%. Found: C, 51.35%; H, 2.13%.

Results and discussion

Synthesis

As shown in Scheme 1, the dimer **3** was synthesized by the Stille coupling reaction between 5-bromodithieno[2,3-*b*:3′,2′-*d*]thiophene and monostannyl dithieno[3,2-*b*:2′,3′-*d*]thiophene **7** derivatives with $Pd(PPh_3)_4$ as catalyst. The vinylene-bridged dimer **4** was achieved by low-valence titanium-mediated McMurry coupling from dithieno[3,2-*b*:2′,3′-*d*]thiophene-2-carbaldehyde **10**. However, the vinylene-bridged dimer **6** was synthesized using the Wittig reaction. Monoalcohol **8**, obtained by reduction of dithieno[2,3-*b*:3′,2′-*d*]thiophene-5-carbaldehyde with $NaBH_4$, was treated with triphenylphosphonium bromide in refluxing CH_3CN to yield phosphonium salt **9**. A Wittig reaction between compounds **9** and **10** in the presence of t-BuOK gave compound **6** in a high yield at room temperature. Compounds **3**, **4** and **6** were slightly soluble in common organic solvents and purified by sublimation. The compounds were characterized by MS and elemental analysis and the results were consistent with the predicted chemical structures.

Optical, electrochemical and thermal properties

The thermal properties of the fused-ring dimers were investigated by thermogravimetric analysis (TGA) and differential scanning calorimetry (DSC). The thermal properties, including melting points (T_{DSC}) and 5% weight loss temperatures (T_{deg}), of these molecules are shown in Table 1. According to TGA analysis, all the compounds are thermally stable, at least up to 320 °C under a nitrogen atmosphere. The compounds **1–6** show melting points ranging from 218 °C to 338 °C with dimers **3** and **6** the lowest (218 °C and 260 °C) and dimer **5** at the highest (338 °C), which imply weaker intermolecular interactions in compounds **3** and **6**, and stronger intermolecular interactions in compound **5**.

To explore the correlation between solid-state optical behavior and packing arrangement, absorption spectra of all the compounds in THF solution and as thin film (deposited on quartz) were measured. Table 1 summarizes the optical properties of compounds **1–6**. It is generally recognized that α-linked fused and non-fused ring oligothiophenes with an equal number of double bonds have similar longest-wavelength absorption.[35] However, directly linked dimers **1**, **2** and **3**, which have six double bonds but different fused ring units, have markedly different absorption λ_{max} values. Compared to compound **1**, the absorption maxima of **2** and **3** are blue shifted by 45 nm and 22 nm, respectively. The optical data show that the dithieno[2,3-*b*:3′,2′-*d*]thiophene unit causes a blue shift by *ca.* 22 nm in directly

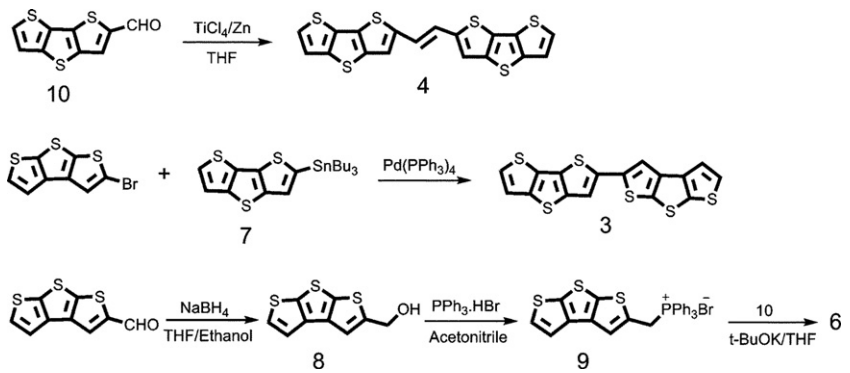

Scheme 1 Synthesis of target molecules **3**, **4** and **6**.

Table 1 Thermal, optical, and electrochemical properties of dimers of dithienothiophenes

Compound	T_{deg}[a][°C]	T_{DSC}[b][°C]	λ_{max}[nm] solution[c]	λ_{max}[nm] thin film[d]	E_{HOMO}[e][eV]	E_g[f][eV]	E_g[g][eV]
1	335	316	390	327, 338	5.43	2.80	2.36
2	333	256	345, 403	379, 403	5.49	3.15	2.63
3	335	218	368	364	5.46	2.93	2.41
4	336	318	415, 439	349, 362, 470	5.33	2.65	2.24
5	342	338	379, 398	339, 423	5.39	2.91	2.48
6	320	260	396, 417	383, 448	5.36	2.76	2.39

[a] Degradation temperature (T_{deg}) determined by TGA corresponding to 5% weight loss at 10 °C min^{-1} under nitrogen flow. [b] Melting point determined by DSC with a scan rate of 10 °C min^{-1}. [c] Measurement performed in THF solution. [d] 50 nm thick film deposited by vacuum on quartz. [e] E_{HOMO} determined by cyclic voltammetry (CV) in THF solution. [f] E_g estimated according to the onset of UV absorption in THF solution. [g] E_g estimated according to the onset of UV absorption in thin films.

linked dimers and by *ca* .18 nm in the vinylene-bridged dimers when compared with the dithieno[3,2-*b*:2′,3′-*d*]thiophene unit. The difference in the degree of absorption maxima shift can be attributed to the fact that the conjugation is limited by the central cross-conjugated double bonds in the dithieno[2,3-*b*:3′,2′-*d*]thiophene unit.[32] As expected, vinylene-bridged dimers **4**, **5** and **6** have longer conjugation lengths than those directly linked analogues (compound **1**, **2** and **3**), with a corresponding red shift in the absorption spectra (Fig. 2). Typically, the conjugated oligomers and polymers are red shifted in the solid state relative to solution due to the chromophore adopting a more planar conformation which results in an increase in the effective conjugation length.[36,37] However, the spectra of most thiophene-based oligomers are blue shifted compared to those obtained in solution indicating that the intermolecular interactions play a major role in determining the solid state optical properties.[38,39] Accordingly, compounds **1**, **4** and **5** display large blue (40–50 nm) shifts in absorption spectra in the solid state compared to solution, while the spectrum of compound **2** is red shifted. The blue shift may be due to exciton coupling between adjacent molecules, which have their long axes parallel (H aggregation) and the red shift may result from the face to face intermolecular interactions (J aggregation). In the case of compound **6**, the absorption spectrum in the solid state becomes broadened with a blue shift by 12 nm and a red shift by 30 nm relative to solution. This indicates that there are different types of interactions in the thin film (H aggregation and J aggregation). However, the thin film spectrum of compound **3** is blue shifted by only 4 nm, which is indicative of a weak splitting of the excited level.

The electrochemical properties of these compounds were investigated by cyclic voltammetry (CV) studies, performed under nitrogen in 0.1 M $TBAPF_6$/THF solutions with a scan rate of 100 mV/s. With the exception of compound **5**, all the systems show one quasi-reversible oxidation wave within the span of the solvent-electrolyte window; data are summarized in Table 1. The highest occupied molecular orbital (HOMO) energy levels, estimated from the oxidation onset, vary from 5.3 to 5.5 eV and the HOMO–LUMO gaps obtained from the absorption onsets vary from 2.6 to 3.2 eV. Judging from these data, we expect that all the compounds are stable semiconductors. It is interesting to note that by replacing a dithieno[3,2-*b*:2′,3′-*d*]thiophene with a dithieno[2,3-*b*:3′,2′-*d*]thiophene unit, the HOMO levels are shifted by *ca*. 0.03 eV. We suggest this phenomenon arises mainly from the reduced electron delocalization from dithieno[2,3-*b*:3′,2′-*d*]thiophene in comparison with dithieno[3,2-*b*:2′,3′-*d*]thiophene and the ethylene units cause a lowering by *ca*. 0.1 eV compared to directly linked analogues.

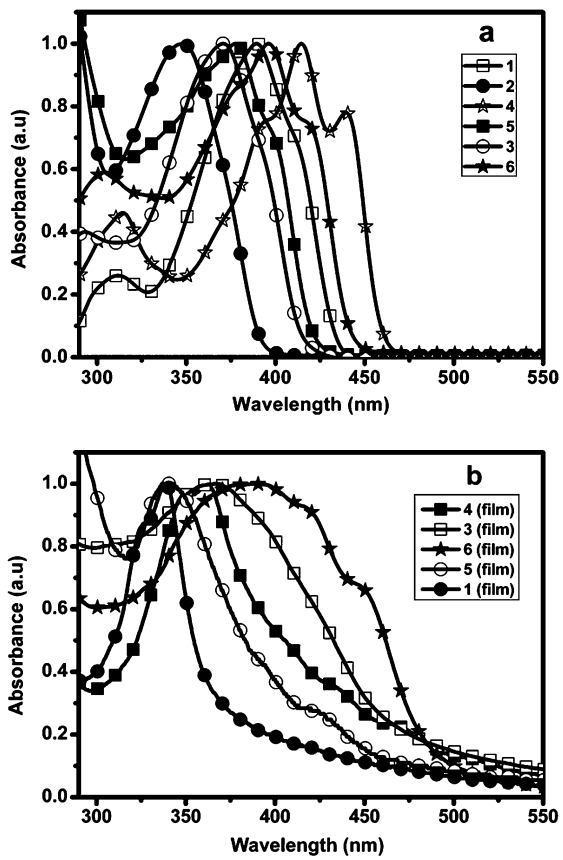

Fig. 2 Optical absorption spectra of the dimers in THF solution (a) and in the thin films (b).

Crystallographic analyses

A single crystal of compound **4** was obtained from toluene/THF solution at room temperature and analysed by X-ray diffraction; crystallographic details can be found in ESI.† Fig. 3 shows the crystal structure and packing motifs of compound **4**. The compound is nearly planar with an anti conformation of two dithieno[3,2-*b*:2′,3′-*d*]thiophene units, which is somewhat similar to that of compound **1**.[24] In fact, the molecular crystallographic structure and the arrangement of compound **4** are strikingly different to those of compound **1**. This molecule crystallizes in $P2_1/n$ space group and packs having a 13.55 Å inter-columnar repeat distance. When viewed down the *b*-axis, the molecules are π stacked (interplanar distance of 3.51 Å) in two nonequivalent stacks that are nearly vertical to each other (*ca*. 84°) due to the occurrence of C–H···π intermolecular contacts (range from

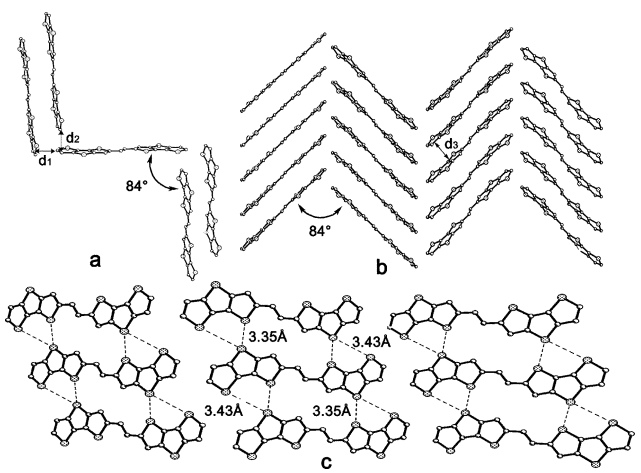

Fig. 3 (a) View of the interstack contacts of compound **4**; $d_1(C\cdots H) = d_2(C\cdots H) = 2.73$ Å. (b) View down the crystallographic *a*-axis; $d_3(\pi\cdots\pi) = 3.51$ Å. (c) View down the crystallographic *b*-axis. Hydrogen atoms are omitted for clarity.

2.37 to 2.86 Å), resulting from the lower C/H ratios in the molecule.[20] The molecules within a given stack are tilted *ca*. 42° with respect to the stacking axis, causing the molecules to assume a "staircase" structure (Fig. 3(b)) when viewed along the *b*-axis. The packing motifs are most likely to be attributed to the existence of S···S interactions and C–H···π interactions. It should be noted that the strong intermolecular interactions between nonequivalent molecules in adjacent stacks lead to a larger Davydov splitting in the optical spectra for the solid form of compound **4** (see ESI†).

Film microstructure and morphology

To investigate the crystalline order of the ring-fused dimers, X-ray diffraction (XRD) patterns were obtained on 60 nm films deposited at different temperatures on octyltrichlorosilane (OTS) treated substrates. The X-ray diffraction pattern of a thin film of **1** deposited on an OTS-SiO_2/Si substrate at room temperature is shown in Fig. 4a. The positions and intensities are in good agreement with experimental results reported by Holmes.[40] It indicates that there is no change in orientation and crystallinity of the thin films when the substrate temperature changes. The corresponding film *d*-spacing (16.5 Å) is one-half of the unit cell *a* axis, meaning that the molecules are oriented with their long axis parallel to the substrate normal, with a tilting of ~0°. This stacking is favourable for charge carrier transport due to the direction of face to face interactions parallel to the substrate surface. For the XRD spectrum of **4**, deposited at 27 °C, there exists one dominant set of Bragg reflections up to fourth-order reflections ($2\theta = 9.60°, 12.76°, 19.26°, 24.16°$), which correspond to the (0 0 *k*) plane of the single crystal, revealing a high crystalline structure in the thin film. The *d*-spacing (9.2 Å) calculated from the primary peak is nearly one-half of the molecular length, indicating the long molecular axis is parallel to the substrate normal, with a tilting of 60°. There is also a second set of reflection peaks at 14.20° corresponding to a *d*-spacing of 4.6 Å, suggesting the existence of two crystalline phases or two different orientations normal to the substrate surface. For compound **5**, the film is also characterized by a very high degree of texture. Based on the X-ray crystallographic analysis, the molecule is nearly orthogonally oriented onto the substrate, an orientation well known to achieve high carrier mobility due to the intermolecular interactions parallel to the direction of the channel current flow.[41] In the case of **2**, two peaks at $2\theta = 10.9°$ and 16.4° are observed, indicating the existence of two morphologies. However, there is no peak in the XRD patterns of **3** and **6**, indicating that the films are amorphous and the molecules are randomly oriented in the thin films. The morphologies of vacuum-deposited thin films under different substrate temperatures were investigated by atomic force microscopy (AFM). As shown in Fig. 4b and d, the morphologies of **1** and **4** are found to be smooth with rather large crystallites. However, the

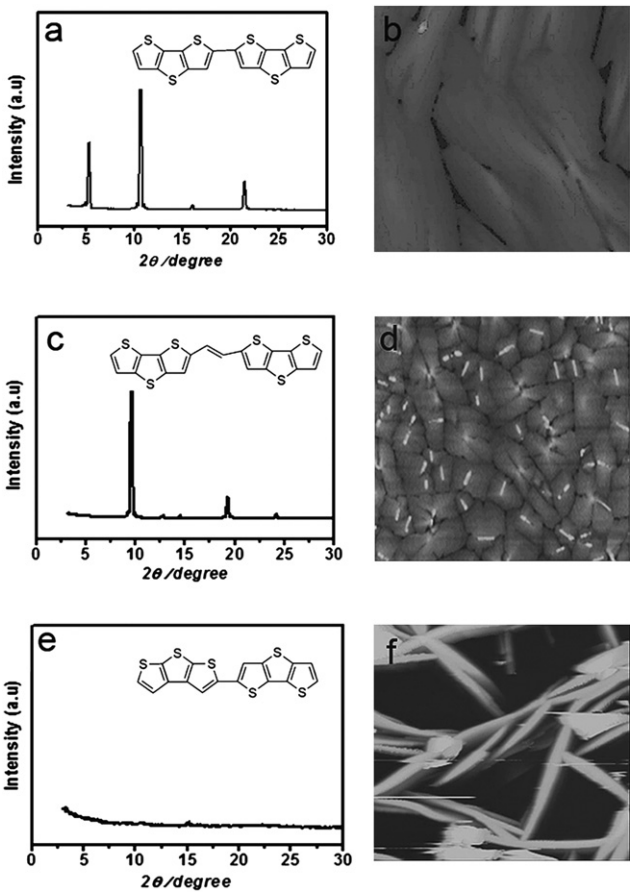

Fig. 4 XRD patterns of 60 nm thick thin films vacuum deposited on OTS-treated Si/SiO_2 at different temperatures: a, b) compound **1** (27 °C); c, d) compound **4** (27 °C); e, f) compound **3** (27 °C).

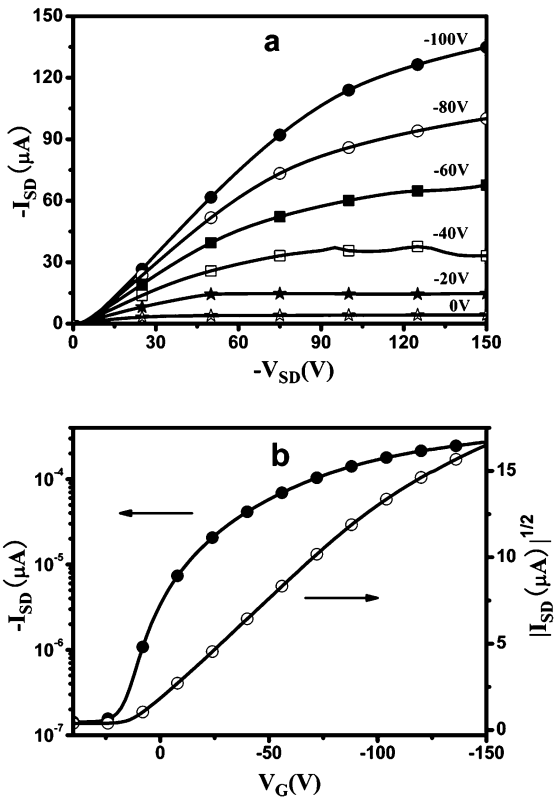

Fig. 5 Plots of source–drain current *versus* source–drain voltage characteristics of the thin films OFETs of **4** deposited at 50 °C (a); transfer characteristics of the devices (b).

Table 2 FET characteristics of fused-ring dimers prepared by vacuum-deposition on OTS treated substrate surfaces (60 nm) at different temperatures[h]

	27 °C		40 °C		60 °C		80 °C		100 °C	
Compound	μ($cm^2V^{-1}s^{-1}$)	on/off	μ($cm^2V^{-1}s^{-1}$)	on/off	μ($cm^2V^{-1}s^{-1}$)	on/off	μ($cm^2V^{-1}s^{-1}$)	on/off	μ($cm^2V^{-1}s^{-1}$)	on/off
1	0.05	10^3	0.07	10^3	0.05	10^3	0.03	10^3	0.03	10^4
4	0.08	10^3	0.07	10^3	0.07	10^3	0.03	10^3	0.05	10^3
5	0.42	10^7	0.37	10^6	0.12	10^6	0.002	10^7	0.012	10^7

[h] Average mobilities and on/off ratios of 10 devices.

morphology of **4** is less regular with more grain boundaries than that of **1**, partially due to two crystalline phases present in the film. On the other hand, the AFM image of the film from **2** shows highly intermingled, small squared-shaped grains with rough morphology and the film of **3** consists of elongated grains with very poor connectivity. Films of **5** reveal a 2D layered morphology with larger sized crystallites and fewer grain boundaries, favorable structures for high carrier mobility. These results are consistent with the characteristic structures observed in XRD patterns.

Thin-film transistor device fabrication and characterization

OFETs were fabricated by vacuum deposition on OTS treated Si/SiO_2 at different temperatures and gold electrodes (60 nm) were deposited by using shadow masks with W/L of 5.3 mm/100 μm. All the devices were studied under ambient conditions and displayed p-type properties in air.

Fig. 5 shows the drain/source (I_{DS}) current and square root of I_{DS} *versus* gate voltage (V_G). The hole mobility calculated in the saturated regime, and the on/off ratios obtained at different temperatures, are summarized in Table 2. The thin film OFETs of compound **1** fabricated at different temperatures on OTS-treated Si/SiO_2 are similar to the values (0.03–0.05 $cm^2V^{-1}s^{-1}$) of semiconductors vacuum deposited on HMDS-treated Si/SiO_2 substrates, measured in a N_2 atmosphere.[24,40] However, the on/off ratio is about five orders of magnitude lower than those obtained with HMDS-treated substrates. The low on/off ratios may be associated with some unfavorable interactions with the dielectric surface, which can be improved by applying different dielectric surface treatments.[42,43] For compound **4**, the charge mobility within the devices is in the range of 0.03–0.08 $cm^2V^{-1}s^{-1}$; the best performance is obtained at $T_s = 20$ °C, with a mobility of 0.08 $cm^2V^{-1}s^{-1}$, an on/off ratio of 1.9×10^3, and a threshold voltage of −14 V. As shown in Table 2, there is only a slight change in μ at elevated temperatures. It seems that the temperature has a limited effect on the molecular orientation and/or crystallinity of the thin films. Although the performance behaviors of **1** and **4** are similar, it is difficult to explain the results due to the differences between morphologies of their thin films, single-crystal arrangement and solid state interactions. In the case of **2**, the TFT mobility obtained at $T_s = 20$ °C is 0.005 $cm^2V^{-1}s^{-1}$, which is lower by 1 order of magnitude as compared to the corresponding devices of **1** and **4**. The inferior FET characteristics are related to the less efficient packing arrangement (sandwiched herringbone structure), in which the hole is often trapped, and only occasionally escapes from the dimers to become an effective carrier.[32] Compound **5** exhibits excellent device performance, with a mobility as high as 0.47 $cm^2V^{-1}s^{-1}$, an on/off ratio up to 10^7 at room temperature and an improved mobility of up to 0.89 $cm^2V^{-1}s^{-1}$ by a two-stage process. This study shows that the FET performance of compound **5** is clearly better than those devices obtained with other materials at room temperature. The difference is probably due to the compressed packing mode of compound **5** combining multiple intermolecular interactions, which play a major role in this considerable improvement.[32] However, the mobility decreases with increasing substrate temperature. This trend is likely due to different thermal expansion coefficients between the semiconductor and the substrate, which result in cracked films at high temperatures. On the other hand, the two asymmetric molecules **3** and **6** exhibit a low mobility on the order of 10^{-4} $cm^2V^{-1}s^{-1}$, strong disorder in molecular packing resulting from the asymmetric structures, and cracked amorphous films are the likely explanations.

Conclusion

We have synthesized a series of semiconductor materials based on the directly linked and vinylene-bridged dimers of dithienothiophenes. A comparative analysis of the optical absorption, thermal properties, electrochemical potentials, and film morphologies of these systems has shown that the molecular packing motifs and intermolecular interactions have a major effect on the device performance. This study reveals that the dithienothiophene units are ideal building blocks for designing stable organic semiconductor materials with good device performance. An appropriate combination of dithienothiophenes can form well-organized molecular packing in thin films that results in good device performance. For example, the vinylene-bridged dimers **4** and **5** show mobilities of 0.08 $cm^2V^{-1}s^{-1}$ and 0.89 $cm^2V^{-1}s^{-1}$, respectively. It has also been demonstrated that thin-film morphology, which depends on the nucleation and growth rates in different directions, is very sensitive to molecular structure and well-organized, two-dimensional layered films exhibit high carrier mobility.

Acknowledgements

The authors are grateful for financial support from NSFC(20772131, 20721061), NSFC-DFG joint project TRR61, 973 Program (2006CB932100, 2006CB806200), and Chinese Academy of Sciences.

Notes and references

1 H. E. Katz, *Chem. Mater.*, 2004, **16**, 4748.
2 Y. Sun, Y. Liu and D. Zhu, *J. Mater. Chem.*, 2005, **15**, 53.

3 H. Klauk, M. Halik, U. Zschieschang, G. Schmid and W. Radlik, *J. Appl. Phys.*, 2002, **92**, 5259.
4 H. Meng, M. Bendikov, G. Mitchell, R. Helgeson, F. Wudl, Z. Bao, C. Kloc and C.-H. Chen, *Adv. Mater.*, 2003, **15**, 1090.
5 N. Sakai, G. K. Prasad, Y. Ebina, K. Takada and T. Sasaki, *Chem. Mater.*, 2006, **18**, 3596.
6 B. O. Ong, Y. Wu, P. Liu and S. Gardner, *Adv. Mater*, 2005, **128**, 4911.
7 M. M. Ling and Z. Bao, *Chem. Mater.*, 2004, **16**, 4824.
8 M. Heeney, C. Bailey, K. Genevicius, M. Shkunov, D. Sparrowe, S. Tierney and I. McCulloch, *J. Am. Chem. Soc.*, 2005, **127**, 1078.
9 Z. Bao, A. Dodabalapur and A. Lovinger, *Appl. Phys. Lett.*, 1996, **69**, 4108.
10 H. Sirringhaus, P. J. Brown, R. H. Friend, M. M. Nielsen, K. Bechgaard, B. M. Langeveld-Voss, A. J. H. Spiering, R. A. J. Janssen, E. W. Meijer, P. Herwig and D. M. de Leeuw, *Nature*, 1999, **401**, 685.
11 Y. Li, Y. Wu, P. Liu, M. Birau, H. Pan and B. S. Ong, *Adv. Mater.*, 2006, **18**, 3029.
12 I. McCulloch, M. Heeney, C. Bailey, K. Genevicius, I. Macdonald, M. Shkunov, D. Sparrowe, S. Tierney, R. Wagner, M. W. Zhang, M. L. Chabinyc, R. J. Kline, M. D. Mcgehee and M. F. Toney, *Nat. Mater.*, 2006, **5**, 328.
13 M. Heeney, C. Bailey, K. Genevicius, M. Shkunov, D. Sparrowe, S. Tierney and I. McCulloch, *J. Am. Chem. Soc.*, 2005, **127**, 1078.
14 P. Liu, Y. Wu, Y. Li, B. S. Ong and S. Zhu, *J. Am. Chem. Soc.*, 2006, **128**, 3237.
15 X. Zhang, A. P. Côté and A. J. Matzger, *J. Am. Chem. Soc.*, 2005, **127**, 10502.
16 R. M. Osuna, X. Zhang, A. J. Matzger, V. Hernandez and J. T. L. Navarrete, *J. Phys. Chem. A*, 2006, **110**, 5058.
17 K. Xiao, Y. Liu, W. Qiu, Y. Ma, G. Cui, S. Chen, X. Zhan, G. Yu, J. Qin, W. Hu and D. Zhu, *J. Am. Chem. Soc.*, 2005, **127**, 13281.
18 M. He and F. Zhang, *J. Org. Chem.*, 2007, **72**, 442.
19 Y. Sun, L. Tan, S. Jiang, H. Qian, Z. Wang, D. Yan, C. Di, Y. Wang, W. Wu, G. Yu, S. Yan, C. Wang, W. Hu, Y. Liu and D. Zhu, *J. Am. Chem. Soc.*, 2007, **129**, 1882.
20 A. J. Briseno, Q. Miao, M. Ling, C. Reese, H. Meng, Z. Bao and F. Wuld, *J. Am. Chem. Soc.*, 2006, **128**, 15576.
21 S. T. Bromley, M. Mas-Torrent, P. Hadley and C. Rovira, *J. Am. Chem. Soc.*, 2004, **126**, 6544.
22 J. Xue and S. R. Forrest, *Appl. Phys. Lett.*, 2001, **79**, 3714.
23 M. Miyasaka and A. Rajca, *J. Org. Chem.*, 2006, **71**, 3264.
24 X.-C. Li, H. Sirringhaus, F. Garnier, A. B. Holms, S. C. Moratti, N. Feeder, W. Clegg, S. J. Teat and R. H. Friend, *J. Am. Chem. Soc.*, 1998, **120**, 2206.
25 Y. Sun, Y. Ma, Y. Liu, J. Wang, J. Pei, G. Yu and D. Zhu, *Adv. Funct. Mater.*, 2006, **16**, 426.
26 J. Li, F. Qin, C. Li, Q. Bao, M. B. Chan-Park, W. Zhang, J. Qin and B. S. Ong, *Chem. Mater.*, 2008, **20**, 2087.
27 J. L. Brédas, D. Beljonne, V. Coropceanu and J. Cornil, *Chem. Rev.*, 2004, **104**, 4971.
28 A. Rajca, H. Wang, M. Pink and S. Rajca, *Angew. Chem., Int. Ed.*, 2000, **39**, 4481.
29 A. Rajca, M. Miyasaka, M. Pink, H. Wang and S. Rajca, *J. Am. Chem. Soc.*, 2004, **126**, 15211.
30 M. Miyasaka, A. Rajca, M. Pink and S. Rajca, *Chem.–Eur. J.*, 2004, **10**, 6531.
31 M. Miyasaka, A. Rajca, M. Pink and S. Rajca, *J. Am. Chem. Soc.*, 2005, **127**, 13806.
32 L. Tan, L. Zhang, X. Jiang, X. Yang, L. Wang, Z. Wang, L. Li, W. Hu, Z. Shui, L. Li and D. Zhu, *Adv. Funct. Mater.*, 2009, **19**, 272.
33 L. Zhang, L. Tan, Z. Wang, W. Hu and D. Zhu, *Chem. Mater.*, 2009, **21**, 1993.
34 J. Casado, V. Hernández, O. K. Kim, J. M. Lehn, J. T. L. Navarrete, S. D. Ledesma, R. P. Ortiz, M. C. R. Delgado, Y. Vida and E. Pérez-Inestrona, *Chem.–Eur. J.*, 2004, **10**, 3805.
35 X. Zhang and A. J. Matzger, *J. Org. Chem.*, 2003, **68**, 9813.
36 A. B. Koren, M. D. Curtis and J. W. Kampf, *Chem. Mater.*, 2000, **12**, 1519.
37 T. A. Chen, X. M. Wu and R. D. Rieke, *J. Am. Chem. Soc.*, 1995, **117**, 233.
38 X. Zhang, J. P. Johnson, J. W. Kampf and A. J. Matzger, *Chem. Mater.*, 2006, **18**, 3470.
39 J. Cornil, D. Beljonne, J. P. Calbert and J. L. Brédas, *Adv. Mater.*, 2001, **13**, 1053.
40 H. Sirringhaus, R. H. Friend, X. C. Li, S. C. Moratti, A. B. Holmes and N. Feeder, *Appl. Phys. Lett.*, 1997, **71**, 3871.
41 J. Gao, R. Li, L. Li, Q. Meng, H. Jiang, H. Li and W. Hu, *Adv. Mater.*, 2007, **19**, 3008.
42 Z. Bao, J. A. Rogers and H. E. Katz, *J. Mater. Chem.*, 1999, **9**, 1895.
43 H. Meng, Z. Bao, A. J. Lovinger, B. Wang and A. M. Mujsce, *J. Am. Chem. Soc.*, 2001, **123**, 9214.

